4. EXPERIMENTAL APPARATUS AND TECHNIQUES

4.1 Introduction

The axial load capacity of MV piles is today generally estimated using empirical data assembled from numerous back-analysed pile load tests. In an effort to obtain additional information on the bearing capacity characteristics of this pile type, a laboratory test programme using a model MV pile was carried out as described herein.

A number of model pile tests in sand have been described in the published literature. Some of these include Kerisel (1961 1964), Vesic (1964), de Beer (1963), Przedecki (1975), Clemence and Brummund (1975), Kulhawy et al (1979), Tjechman (1971a, 1971b), Mazurkiewicz (1968), Knabe (1971), Hanna and Tan (1973), Das and Seeley (1976), Robinsky et al (1964) and Robinsky and Morrison (1964). Of the above, the tests carried out by Robinsky and his team, Knabe, Kulhawy and Przedecki were mainly intended to determine soil displacements around a pile while the other references quoted attempted to determine pile capacity. Most of the experiments were conducted with dry sand, and the models used ranged in size from pile shafts of 410mm diameter representing drilled piers (Clemence and Brummund 1975), to 50 to 75mm diameter metal tubes usually representing precast piles (eg Hanna and Tan 1973, Mazurkiewicz 1968). Knabe (1971) investigated pile groups and the influence of the pile cap on the group bearing capacity.

Ideally the model system used to investigate soil/structure interaction should comply with the requirements of dimensional similitude. Prior to setting up a scale model experiment therefore, consideration should be given to the validity of the selected model dimensions, the experimental technique to be used, the properties of the materials involved, and the probable effects of the loads applied and deformations observed.

The limitations of scale models as a means of interpreting prototype pile behaviour, are well recognised (Vesic 1964, 1965, Bassett 1980). Dimensional analysis (Buckingham 1914, 1915, Bridgeman 1931, Langhaar 1951), is one method which may assist in identifying those parts of the model which either do or do not conform to the prototype. Appendix B considers the similitude requirements of a model MV pile using dimensional analysis. The findings of this appendix suggest that the model should be geometrically similar to the prototype, the shear and elastic moduli of prototype and model should be the same, and, most importantly, that the unit weight of the model soil should be scaled in inverse proportion to the linear scaling. Except by the use of, for example, a centrifuge it is unlikely therefore, that on a laboratory scale, the model pile/ soil interaction will properly simulate the prototype.

Nevertheless, model experiments in the laboratory provide virtually the only practicable means of investigating pile behaviour under controlled conditions. And, as Bassett (1980 pg.1) observes, "Any physical model is a prototype in its own right and can be studied as such."

4.2 Model Pile System

Where possible, the model piling system selected for this test programme simulates the prototype in both dimensions and manufacturing technique. The equipment used is shown in Figures 4.1 to 4.10 and plates 4.1 to 4.3. Installation and load testing of these model pile followed the procedures described below. (Reference should be made to Figures 4.1 to 4.3 and plates 4.1 to 4.3.)

A selected sand was "rained" into the glass fronted, steel panelled sand box under a controlled rate of lift to provide an approximately homogenous soil of known uniform density. After flooding the sand box with water, the flat face of the half cone model pile shoe was placed flush against the glass face and then driven into the submerged sand using a drop hammer impacting via packing onto a load calibrated strain gauged drive mandrel. Typical hammer drop heights were of the order of 150mm. A fluid water/cement grout was circulated continuously through the semicircular annulus formed around the drive mandrel during passage of the pile shoe into the soil. At various selected depths of penetration into the sand box, pile head acceleration and driving forces in the mandrel were recorded in order to investigate the effect of depth on the response of the pile to impact. Once a suitable depth of penetration had been reached, similar data was recorded for a final 3 hammer impacts, and large format photographic film exposures (referred to in the following text as "Plates 1 to 3 Dynamic") were obtained of the soil displacements around the pile toe after each recorded impact. Once these tests were completed, and while the grout was still circulating, the pile was load tested to failure to determine the pile toe capacity under static loading conditions.

The grout was allowed to cure in the shaft annulus for a period of fifteen days at which time the pile was load tested to failure by applying the incremental loading technique. Pile head displacements were measured relative to the top of the sand box by placing three dial gauges, accurate to 0,01mm, underneath the pile helmet. The gauges were fixed to magnetic stands which were attached to the top of the steel frame of the sand box. During the test, the output of the mandrel strain gauge groups was recorded and the soil displacements

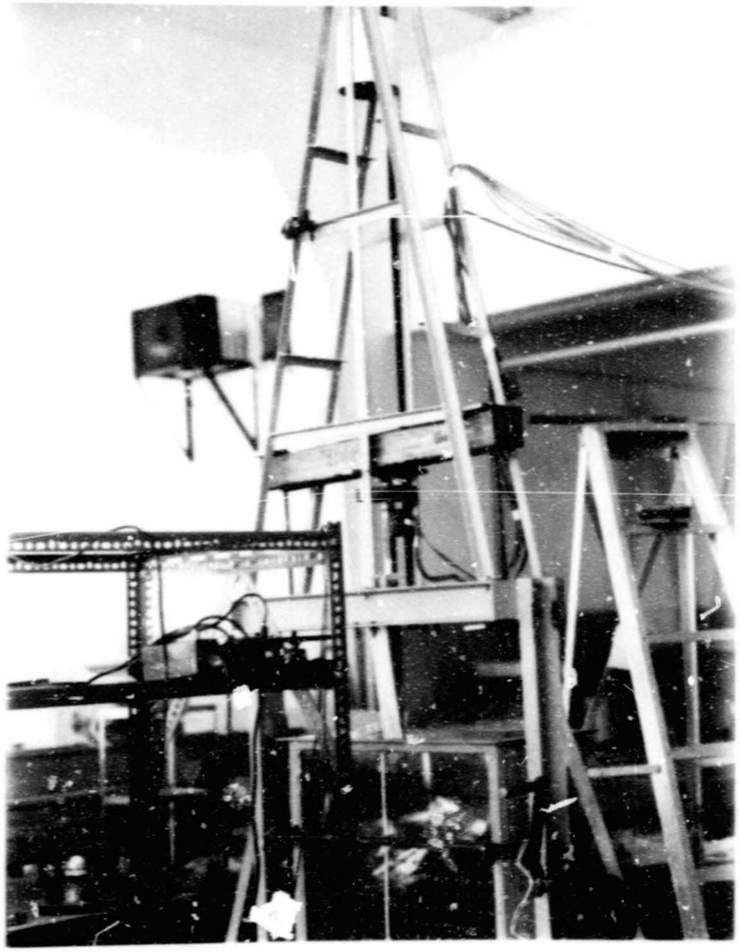

PLATE 4.1a

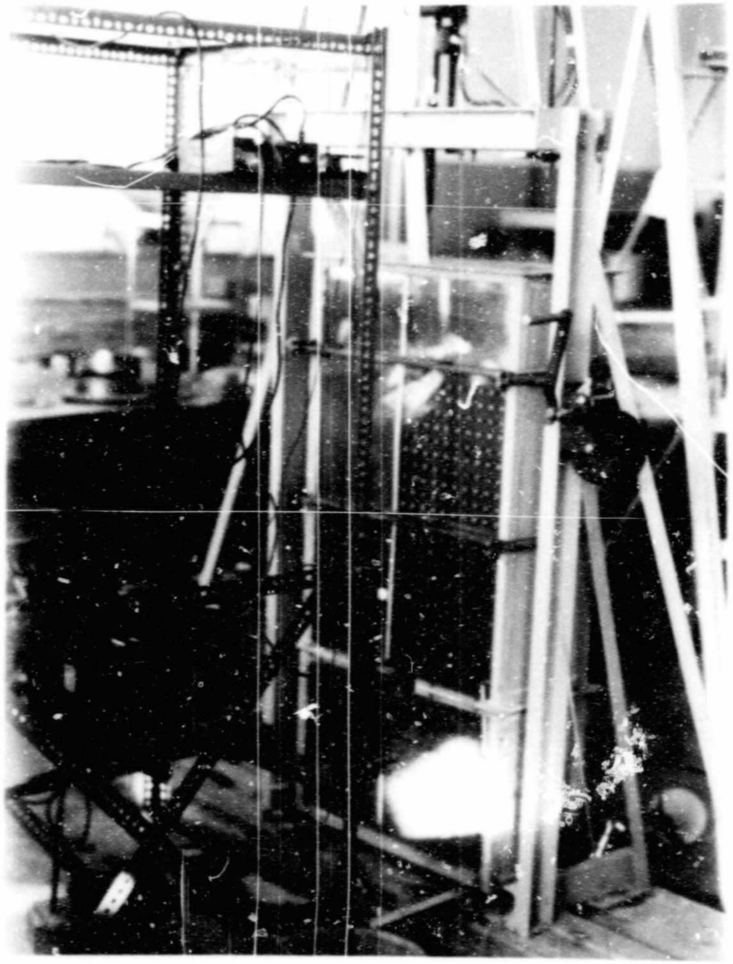

PLATE 4.1b

PLATE 4.1 : General views of pile testing equipment and plate film camera

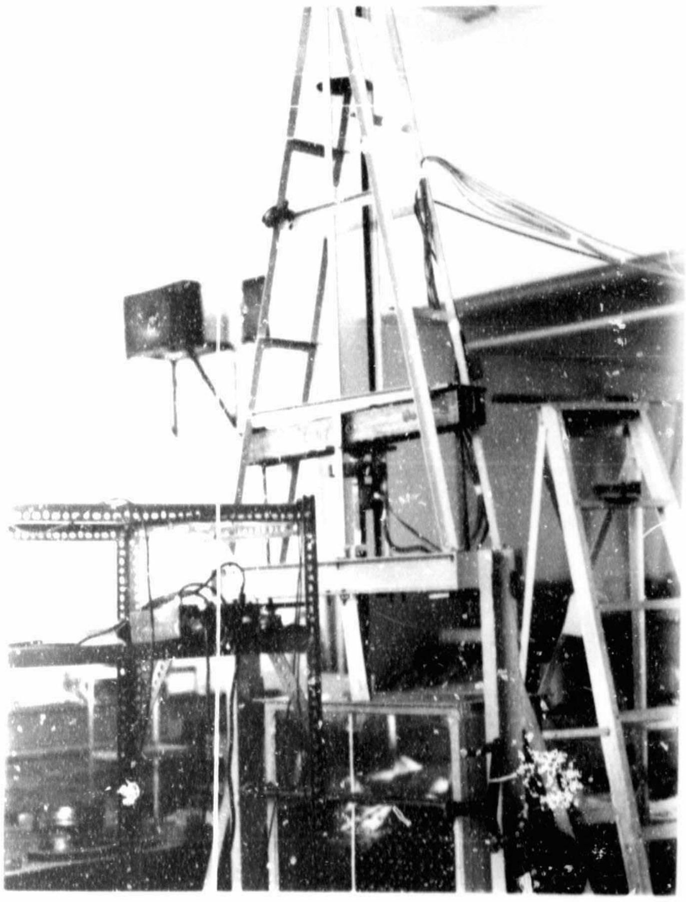

PLATE 4.1a

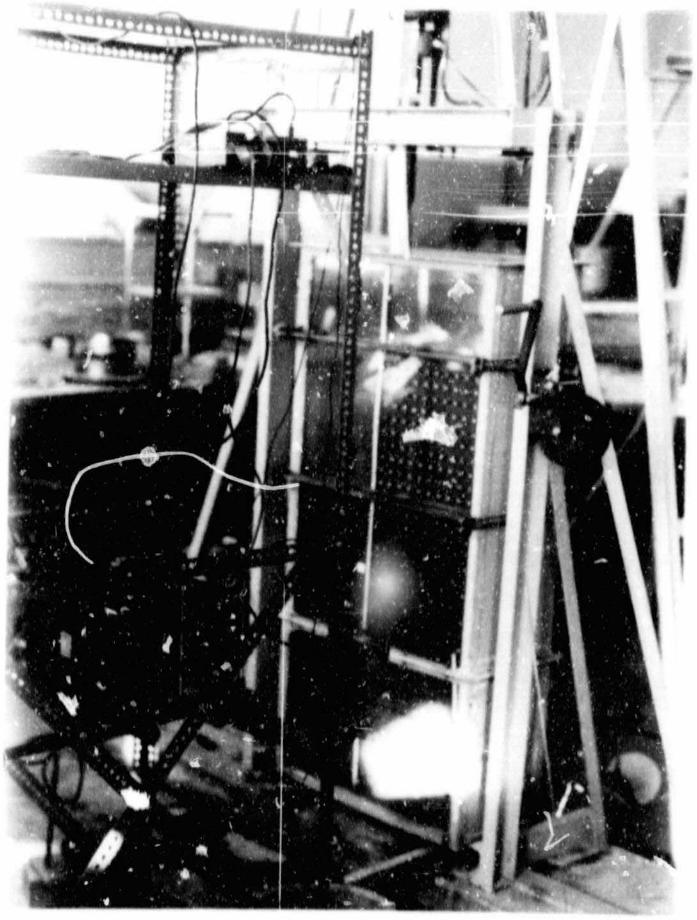

PLATE 4.1b

PLATE 4.1 : General views of pile testing equipment and plate film camera

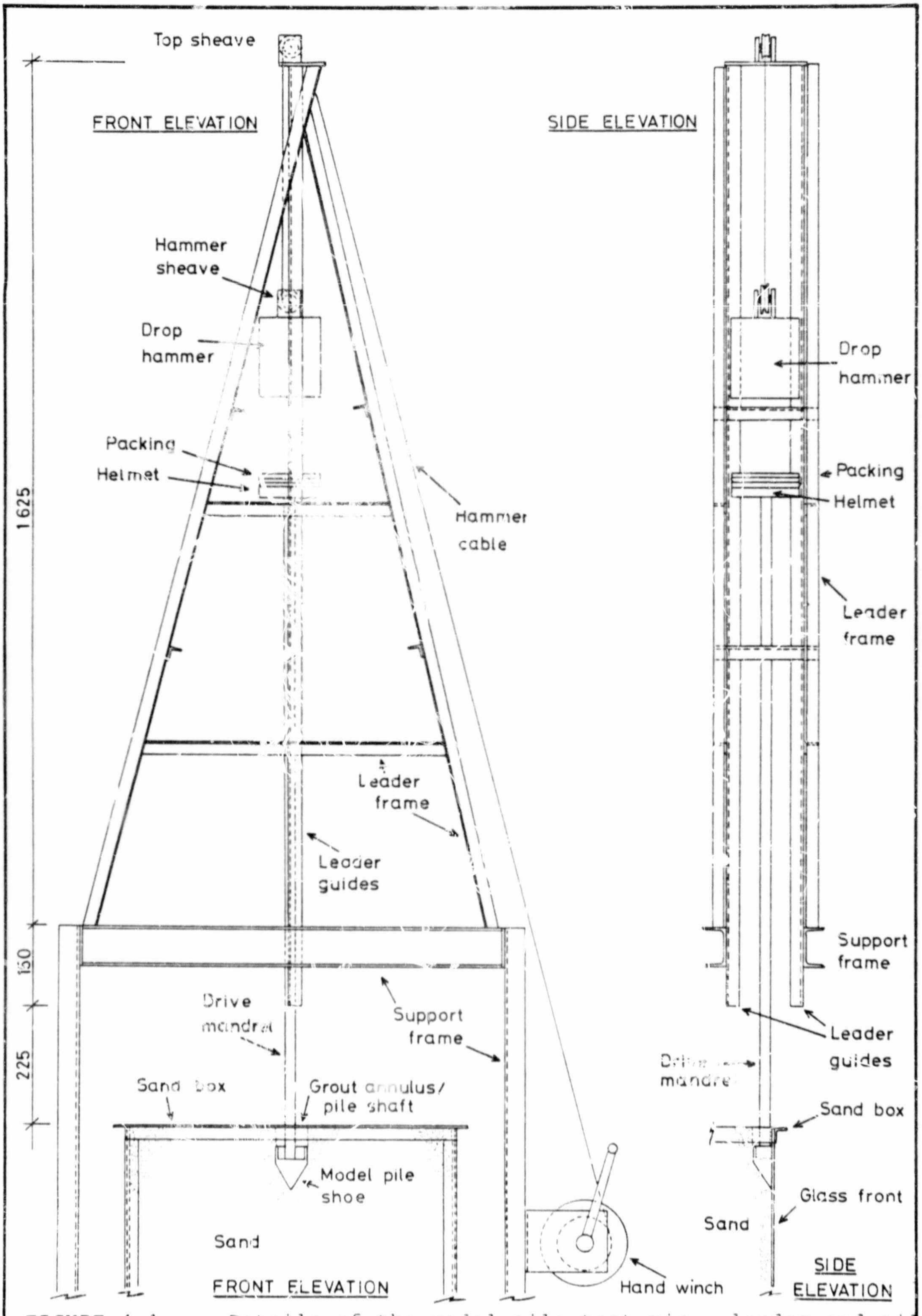

FIGURE 4.1 : Details of the model pile test rig - leader and pile

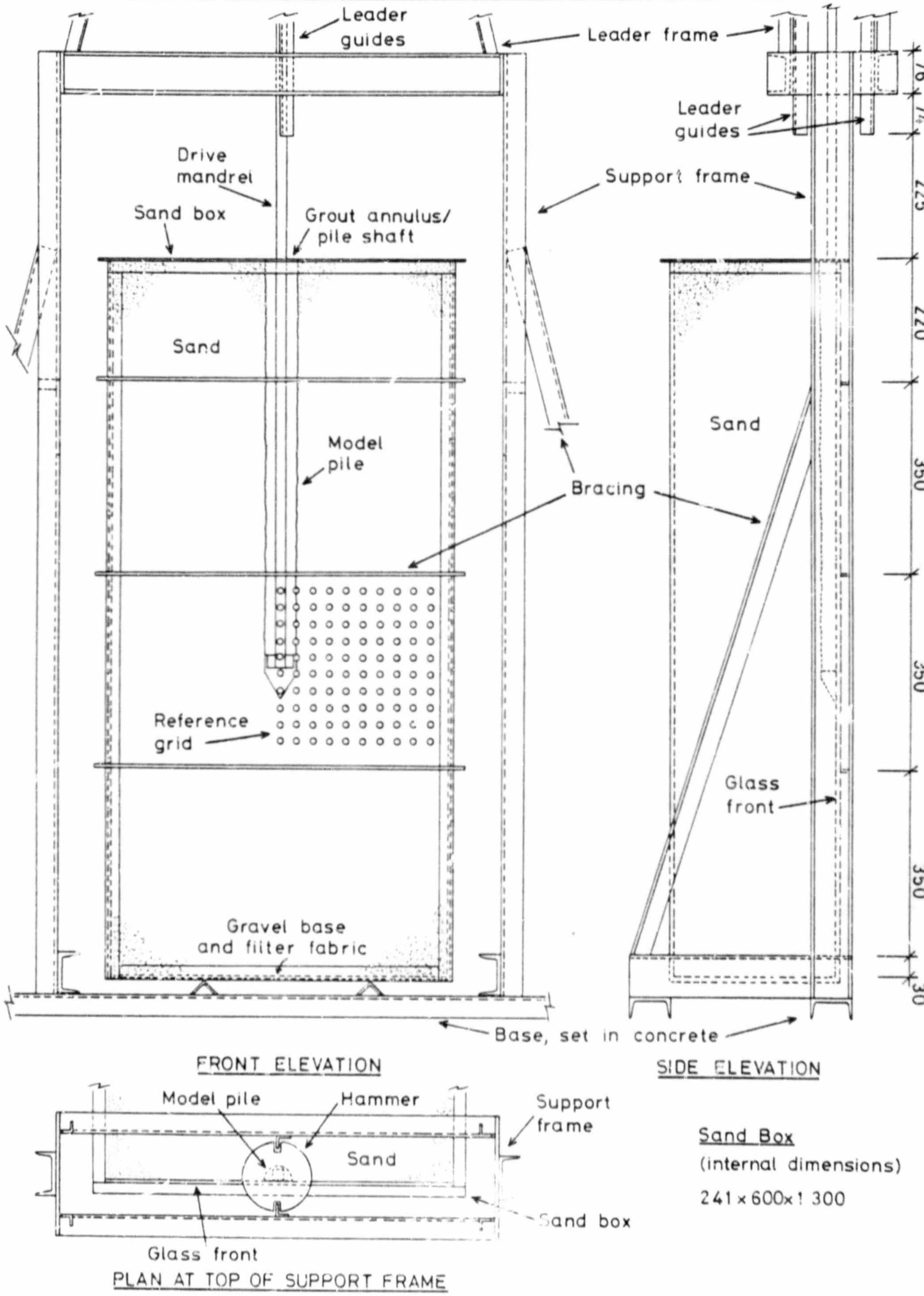

FIGURE 4.2 : Details of the model pile test rig - sandbox

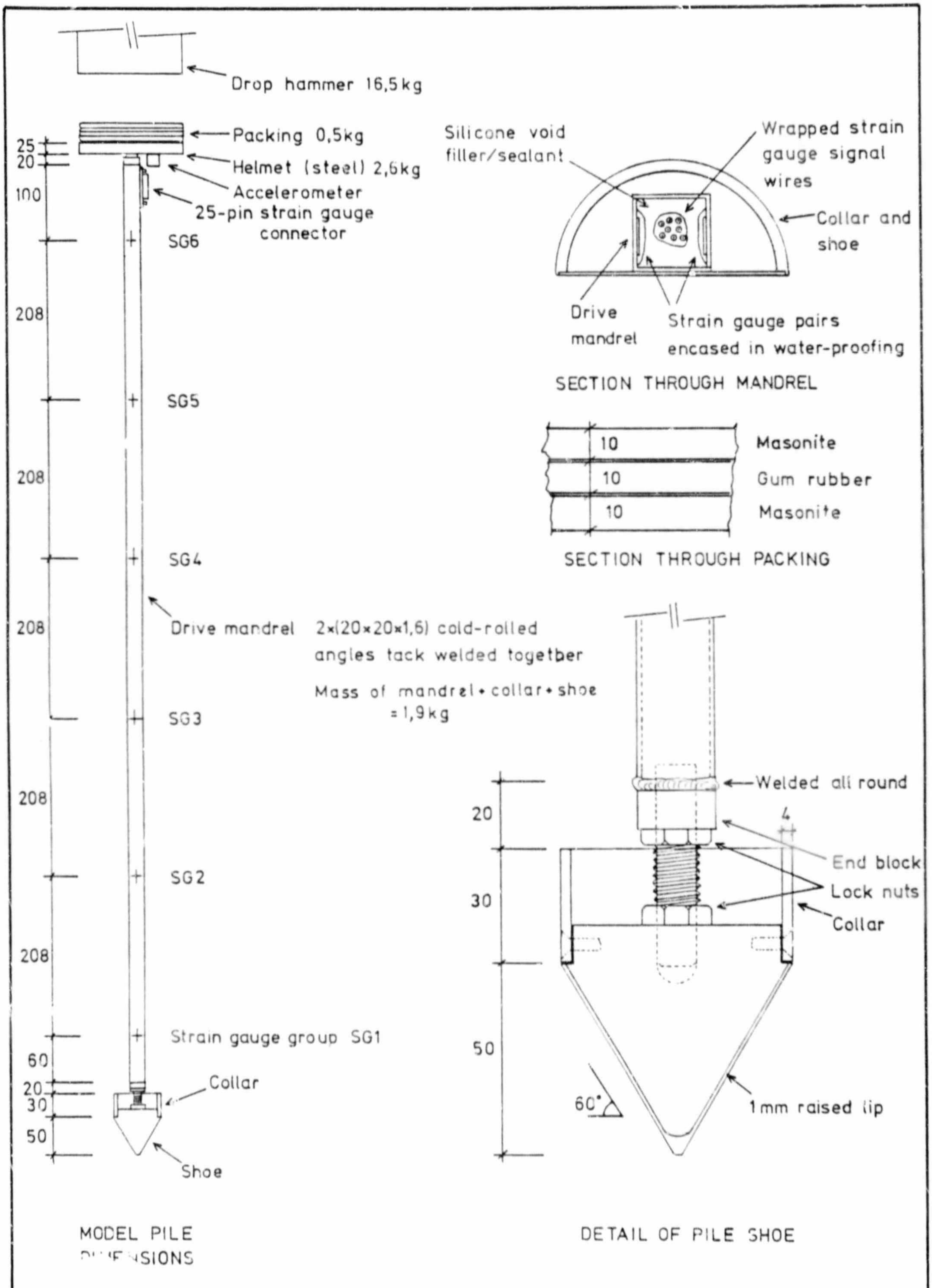

FIGURE 4.3 : Details of the model pile - mandrel and shoe

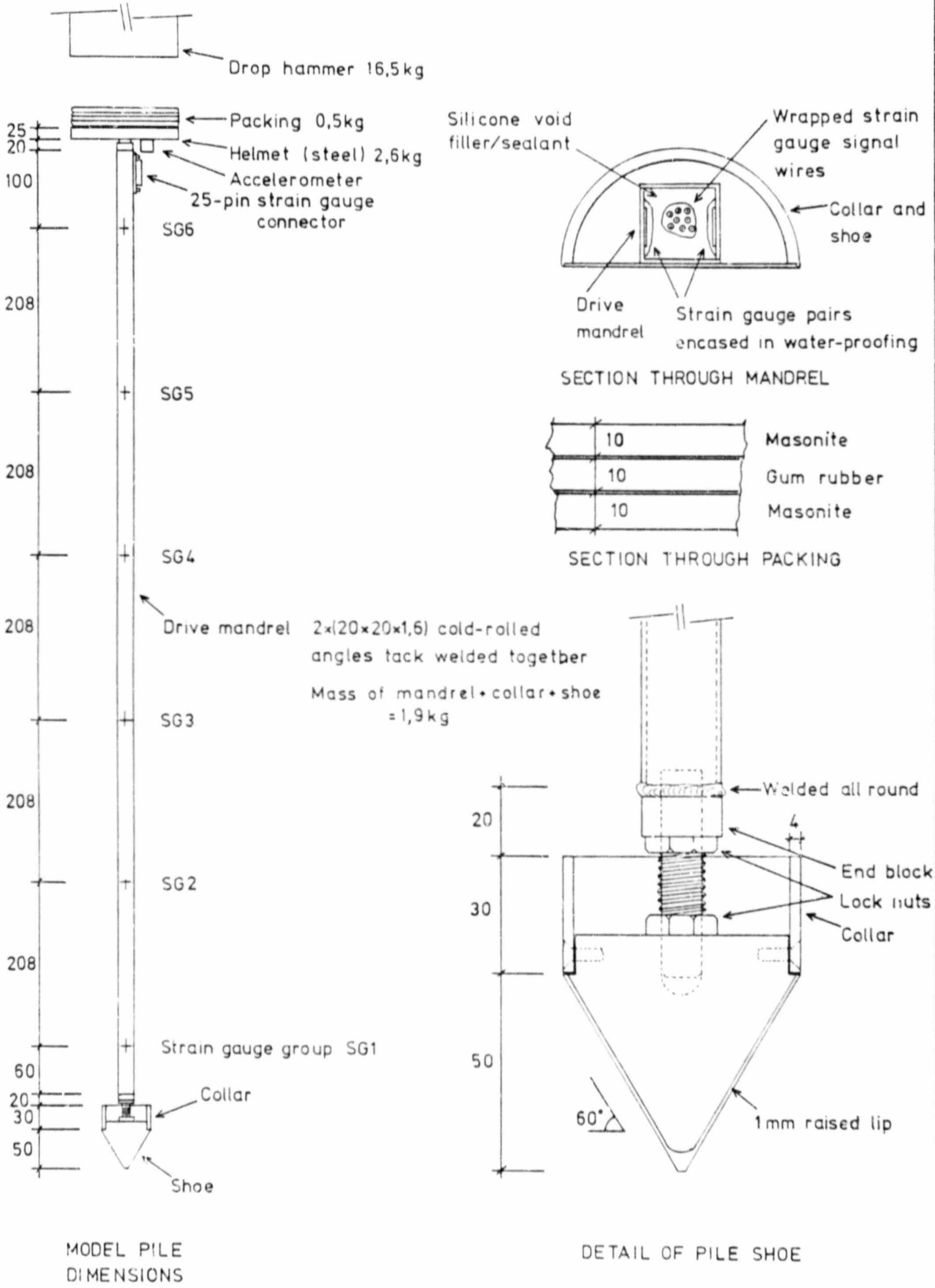

FIGURE 4.3 : Details of the model pile - mandrel and shoe

around the pile toe were again recorded on large format photographic film as a series of exposures, corresponding approximately to the applied load increments. (In the following text these exposures are referred to as "Plates 1 to 4 Static".) In order to obtain load/settlement data on the model pile at higher confining pressures, the sand box was then drained of water, and the load testing to failure procedures and measurements repeated. For this test, however, only a single photographic record of the soil displacements (referred to as "Plate 5 Static") was obtained.

Immediately after this, the pile was removed from the sand box and the output of the strain gauges in the mandrel (now stiffened with grout) recalibrated with respect to load. The unit weight of the moist sand was also determined. The approximate "apparent cohesion" of the moist sand (due to surface tension effects) was obtained by excavating a trench inside the sand box and measuring the limiting height of the freestanding moist sand.

The experimental equipment and procedures described, using a semi-circular half pile driven down the face of a plane glass panel, enabled soil movements to be measured approximately on an axial plane of an axially symmetric model MV pile. Techniques for analysing axially symmetric problems are well known (eg Smith

[1971]). In cases of axial symmetry, soil movements determined in the axial plane on one side of the object are theoretically applicable and precisely similar to any plane lying in the axis of symmetry. It has been assumed throughout this report that the model pile system and the soil displacement data obtained, conformed to an axially symmetric situation. Some of the deviations from this assumption are discussed in Chapter 6 and Appendix A.

Certain aspects of the equipment and procedures described above are discussed in more detail in the following sections.

4.2.1 Details of the Sand Box

The major features and dimensions of the sand box are given in figures 4.2 and 4.1 and portions of it can be seen in Plates 4.1a and b.

The box was manufactured from a welded 25mm angle frame with 6mm mild steel panels welded to the inside of the frame. Overall internal dimensions were 1300mm deep and 268 x 600mm in width. The rear panel of the lower portion of the box was detachable to allow access to the inside of the sand box. When the box was in use the panel was bolted into position with a rubber gasket seal. Before use, the box was coated throughout to prevent rusting. The dimensions of the side panels were such that a 15mm wide groove was formed between the panel edges and the vertical angles in the front of the box. A glass panel, made of three sheets of 4mm thick toughened glass, was slid into this groove to form the front face of the box. A silicone sealant was used to seal the joint and hold the glass in position.

To ensure compatibility of the sand box's internal dimensions with the sand rainer dimensions (see figure 4.6 and 4.7) a spacer plate made of 2mm galvanised sheet with suitable stiffners was placed insi[illegible] [illegible]r face of the sand box. Final internal dimensi[illegible] the sand box were 241 x 600 x 1300mm.

Strip metal stiffners (6mm x 50mm) with 4mm thick rubber spacers inserted between the glass panel and the stiffner were provided at selected depths to prevent excess outward deflection of the glass panel when horizontally loaded.

Access for water to flood and drain the sand box was provided by a valve connected at the base of one of the side panels of the sand box. Inside the box, a layer of coarse sand and gravel covered by a sheet of filter fabric was placed to a depth which just covered the valve orifice.

4.3 The Test Sand

Of the different types of sand available in the Pretoria-Witwatersrand-Vereeniging area, Honeydew Washed Magalies sand was selected as being the most suitable. This is a pale yellow-brown clean siliceous sand (feldspar content approximately 2% by volume) derived by weathering of quartzite. The major portion of the grains are well rounded to subrounded, while the smaller grains are generally flakey to angular. All the grains have a frosted surface.

During preliminary testing of the sand rainer, it became apparent that the dust content of the natural sand could prove to be troublesome. In order to eliminate the dust, the -300 μm portion was separated out and the sand was washed. The +2,0mm portion was also removed. Particle grading curves of both the natural and prepared test sand are given in Figure 4.4. Grading analyses repeated at intervals during the test programme showed that insignificant degradation of the sand occurred during the tests.

The specific gravity of the test sand was measured as 2,634 while maximum and minimum dry densities (obtained following Kolbuszewski and Jones 1961) were measured as 1810kg/m^3 and 1352kg/m^3 respectively. These densities correspond to porosities of 0,315 and 0,487.

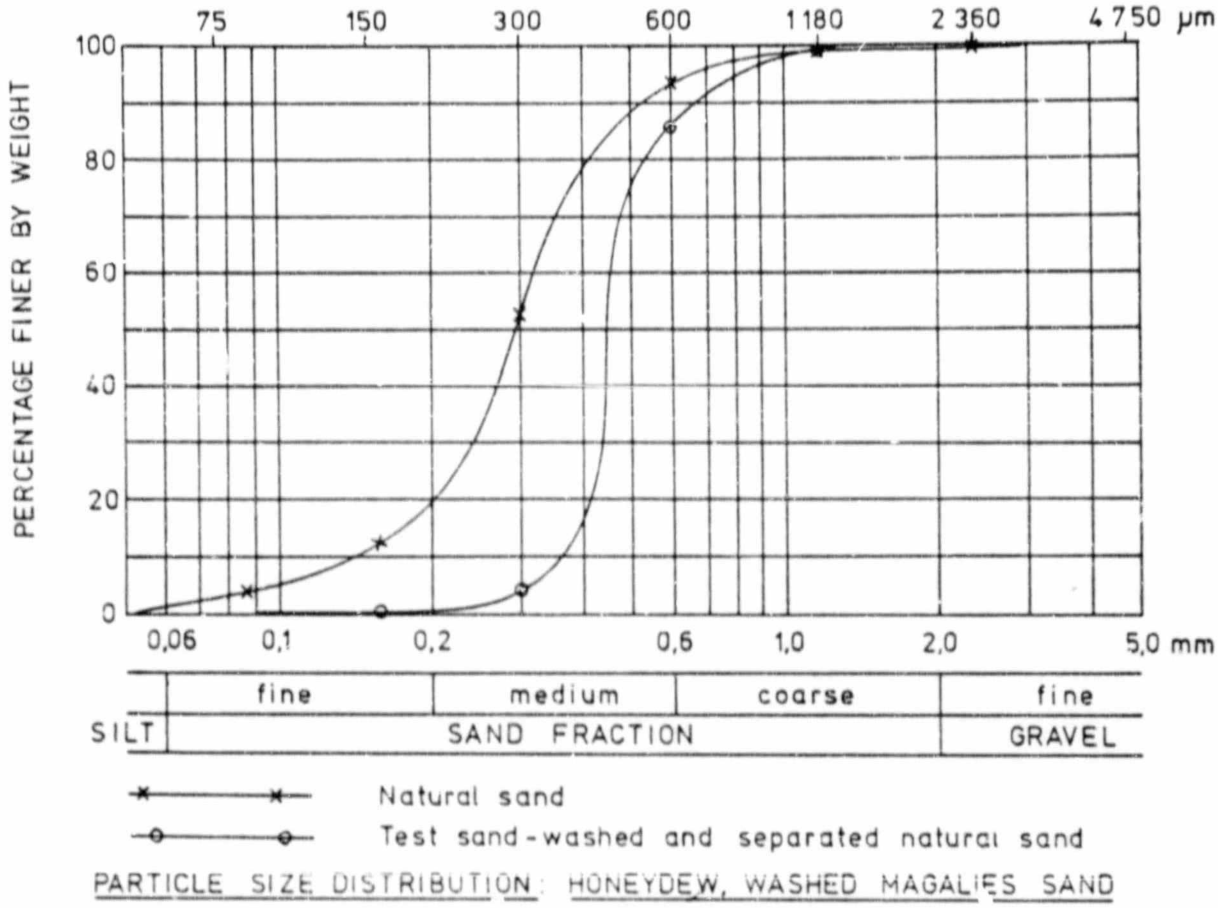

FIGURE 4.4 : Test sand, particle grading curves

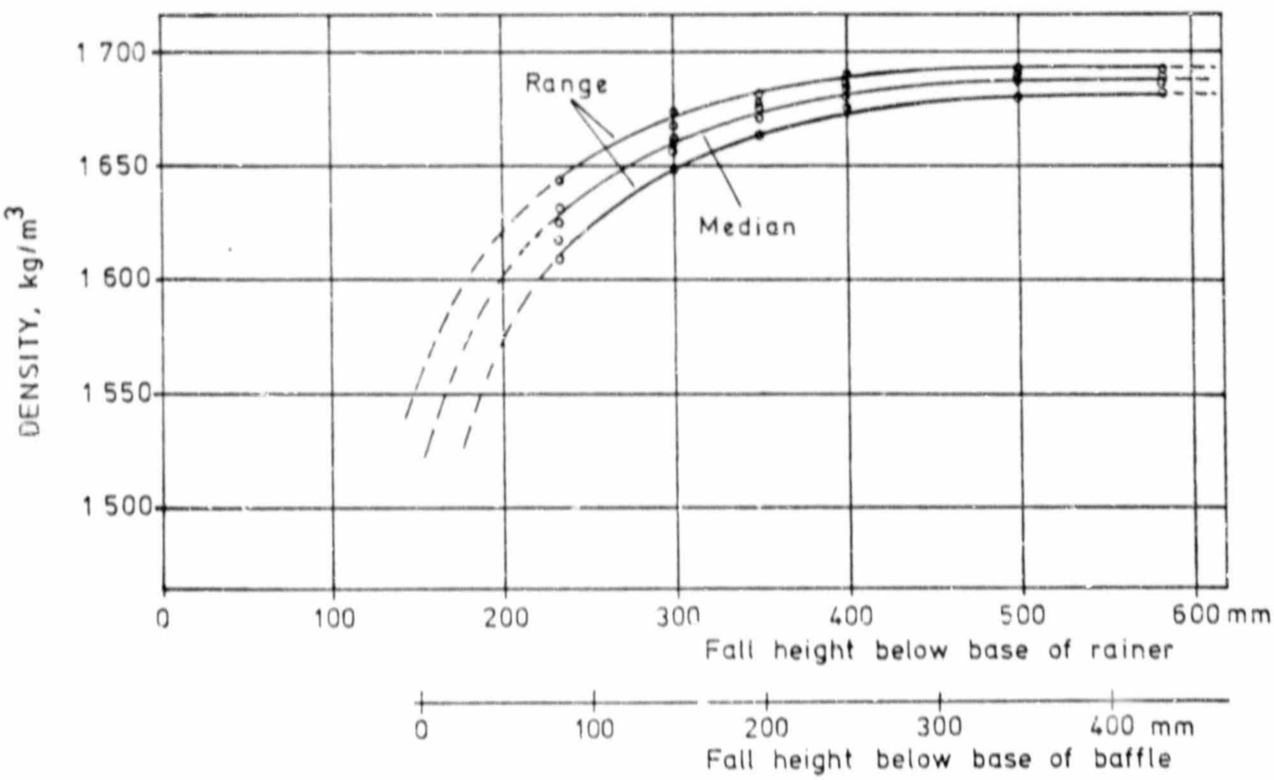

FIGURE 4.5: Relationship between fall height and resulting soil density achieved with the sand rainer

4.4 Sand Placement Technique

Analysis of the performance of full scale pile in natural deposits is frequently complicated by the variable nature of the strata into which they are placed. One of the attractions of model tests is the possible achievement of a uniform model soil. A number of methods for the uniform placement of sand have been proposed (eg Butterfield and Andrawes [1978], Bennett and Gisbourne [1971], Kulhawy et al 1979, Walker and Whitaker 1967, Bieganousky and Marcuson 1976, Vesic 1967). These methods employ a 'raining' technique, in which sand is allowed to free fall into a container from a controlled height. The density of the placed sand is usually related in some way to the fall height and fall rate.

The sand rainer used for this test programme was based on equipment described by Bieganousky and Marcuson (1976). Figures 4.6 and 4.7 show the main details of the rainer. Bieganousky and Marcuson (op cit) recommended a base plate perforation porosity of 1,4%. Tests using a base plate porosity of 1,4% were carried out to check the effectiveness of the sand rainer. These tests showed that, within the enclosed confines of test rig sand box, the air displaced by the falling sand generated a pair of contra rotating vortices which tended to carry the grains laterally resulting in uneven placement of the sand. By halving the base plate porosity to 0,7% and by including a pair of 2,0mm mesh screens (baffles) below the rainer to disperse the sand, an effective raining technique was achieved. Figure 4.5 shows the relationship between fall height and placed dry density obtained with this equipment.

A fall height of 200mm below the base of the bottom baffle of the rainer was selected for this test programme. The rainer was usually filled with about 28kg of sand which rained at an average rate of 7,15kg/min, and approximately 11 lifts were required to fill the sand box. Based on the dimensions of the sand box and the mass of soil used to fill it, the placed soil obtained an average density of 1670kg/m^3 with a range of 20kg/m^3, during a series of 6 test placements. The relative density (RD) was thus 74%, indicating a "dense" sand.

As discussed in section 4.7, the soil displacements around the model pile were measured in a Wild A7 Autograph by tracing the movement of individual grains through a sequence of photographs. To assist in the identification of individual grains about 10% of the sand rained against the glass face of the sand box consisted of particles which had been dyed black. The black grains contrasted strongly with the lighter colour of the un-dyed sand, and could be identified clearly in the photographs.

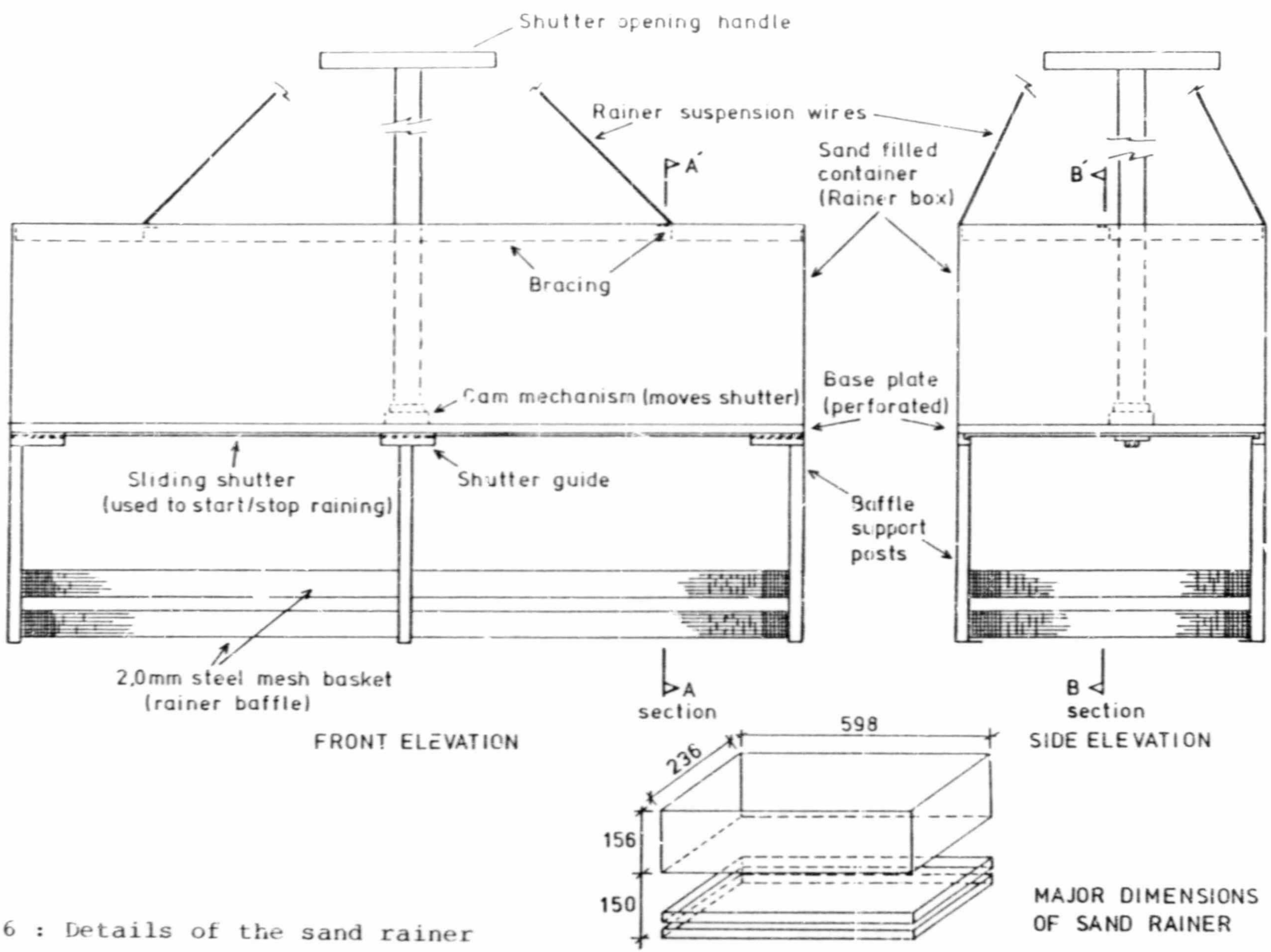

FIGURE 4.6 : Details of the sand rainer

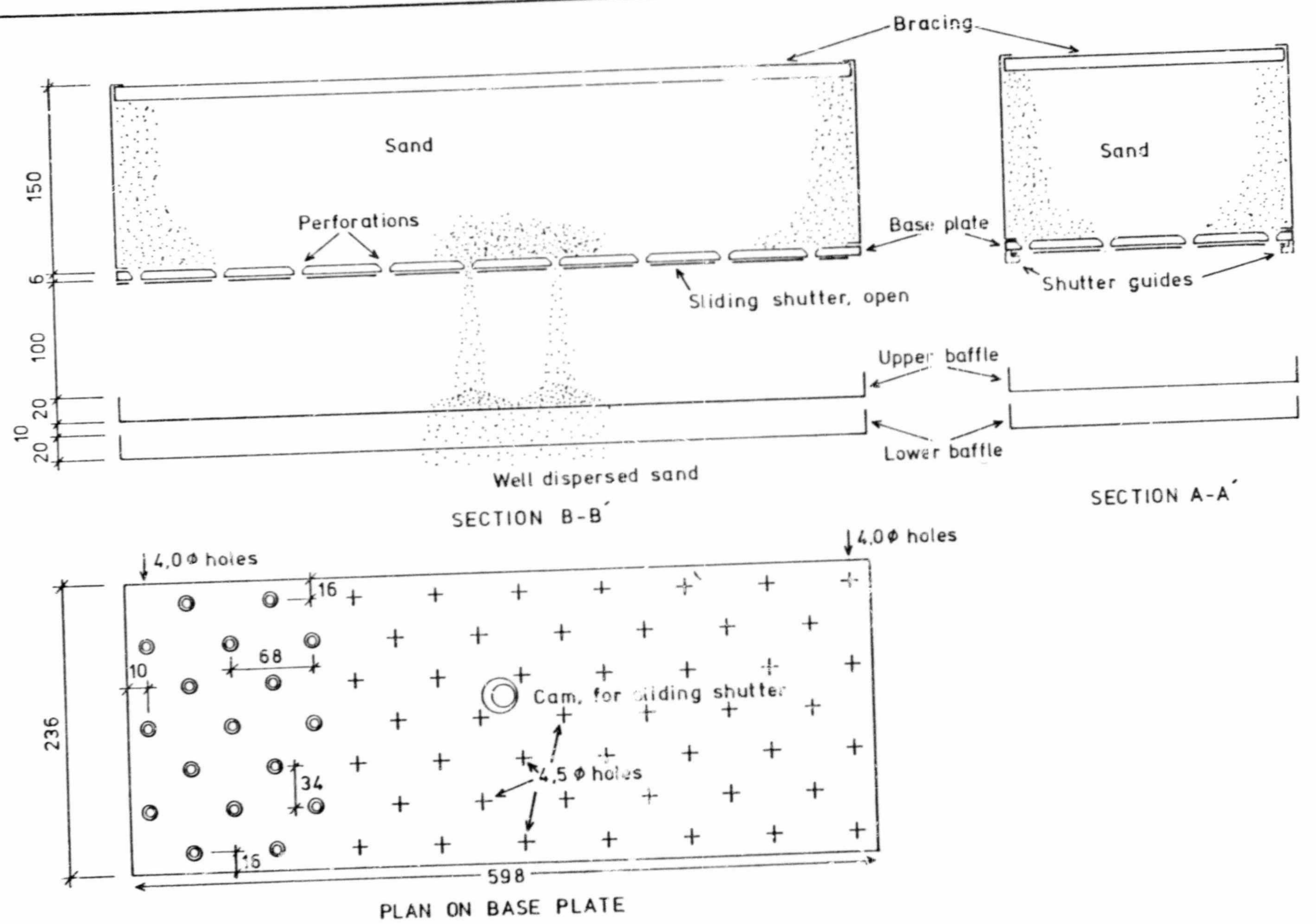

FIGURE 4.7 : Details and principle of the sand rainer

4.5 Model Pile

Details of the model pile and its instrumentation are given in Figures 4.3 and 4.8. The half cone shoe was machined from a solid bar and case-hardened before use. Inclusion of the raised lip around the perimeter of the flat side of the shoe, the portion lying in contact with the glass face of the sand box, assisted greatly in preventing ingress of sand between the shoe and the glass. A number of tests still had to be aborted, however, because of this problem. Allied to this and also critical to the success of an installation test, was correct alignment of the plane of the pile shoe with the glass face of the sand box.

Various types of packing were tested before the combination shown in Figure 4.3 was selected on the basis that the accelerometer and strain gauge outputs under impact, gave smooth oscilloscope traces with no spikes.

4.6 The Model Grouting System

Prototype MV grouts used in the field generally comprise the following components and mix proportions.

Clean coarse siliceous sand	75 kg
Portland cement	50 kg

Water	25.27 l
Tricosal MV (Retarder plasticiser air entraining agent)	525 gms

Using this mix, 28 day cube crushing strengths in the range 25MPa to 35MPa are obtained with grout densities of the order of 2100kg/m^3.

Despite determined attempts to use a similar grout mix in the model tests, (with the sand particle size suitably reduced to the scale of the experiment) separation of the sand from the grout slurry, causing supply pipe blockage, was found to be an erratically persistent problem. The mix proportions eventually selected for the model grout were as follows:

Water	1,75 ℓ	=4,7ℓ
Portland Cement	5,5 kg	
Bentonite	330 gms	
Retarder/Plasticiser Cormix SP4	25 mls	

28 day cube crushing strengths for this mix were typically about 30MPa with a grout density of 2050kg/m^3. Grout prisms, with dimensions of 162,5 x 41,5 x 41,5mm, were used to estimate the elastic modulus of the grout. These gave an average Ec of 17,5 GPa.

Attempts to install the pile into dry sand resulted in a loss of water and consequent stiffening of the grout leading to blockages in the grout pumping circuit. For this reason the model tests were conducted in submerged sand. During the installation of full size MV piles, the grout is usually supplied direct to the annulus above the pile shoe at a rate such that the level of grout in the pile shaft remains constant. Because of the long duration of the model installation tests, however it was found necessary to circulate the grout through the pile shaft continuously. A Mono MWD 30 grout pump with electric motor was used for this purpose and the grout was supplied to the pile through a tube temporarily attached to the drive mandrel. A temporary reservoir was attached to the sand box at the top of the pile to collect the circulating grout and return it to the pump hopper. During pile installation, the grout level inside the reservoir usually rose to about 0,1 m above the top of the sand.

Because wet cement etches and bonds to glass, a method had to be devised to isolate the grout column in the pile shaft from the glass face of the sand box. This was achieved by firstly coating the glass along the line of pile contact with a release agent (Eucon Eucoslip) and secondly by using a tough 300 μm thick plastic (polyamide) strip inserted between the grout and the glass. The strip was cut to the diameter of the pile shoe and to the length of the mandrel, and was permanently formed about its long axis into a curved section with a radius of about 100mm. It was fixed to the pile shoe and aligned parallel to drive mandrel with the convex side towards the pile. This arrangement ensured that frictional contact between the strip and the glass was limited to the strip edges, while the curvature ensured that positive contact was maintained with the glass. A coating of release agent was applied to the concave face of the strip shortly before the model pile was installed.

Despite these precautions, a few sand grains and some cement particles usually managed to enter the space between the strip and the glass. Tests were abandoned if the amount of contamination on this interface was considered excessive. Some comments are given in Section 6.4 and Appendix E on the friction developed at the interface between the pile shaft and the glass front panel.

4.7 Pile Loading System

Plate 4.3 shows the equipment used to apply load to the model pile. This comprised anchor rods which were attached at their lower end to the support frame, with the upper end suspended from a pair of box section reaction beams which straddled the head of the pile. Load was applied to the pile head by screwing a threaded rod against a steel plate saddle placed between the underside of the reaction beams and the steel helmet at the head of the drive mandrel. Both the bottom of the threaded rod and the top of the drive mandrel were machined to provide hemispherical seatings for a ball bearing through which load was applied to the pile.

Loads applied to the pile by this method were measured by the strain gauge group SG6 (see Figure 4.3). Rough control of load application rate could be achieved by monitoring the data from SG6. Dial gauges attached to the sand box were used to record pile head movements.

PLATE 4.2 : Pile loading system

4.8 Data Collection

Measurements on the model pile system provided the following information:

1) Pile head acceleration during impact loading.

2) Shaft load and load distribution during both impact and static loading.

3) Soil displacement around the pile toe and lower shaft during both static and dynamic loading.

Strain gauge bridges attached to the inside of the drive mandrel were used to determine the loads imposed on the pile. The gauges were arranged in full bridge groups aligned orthogonally to the mandrel axis. Leads from the strain gauges were wrapped in metal foil and the surrounding void filled with a silicone sealant as an aid to preventing the access of moisture to the gauges. (See Figure 4.3.) Figure 4.8 gives the details of both the strain gauge and accelerometer instrumentation used. For impact load measurement during pile installation, signal output from the strain gauges had to be amplified in order to produce a measurable oscilloscope trace. A differential input "op-amp" signal amplifier was designed and manufactured by the writer for this purpose. The performance of the

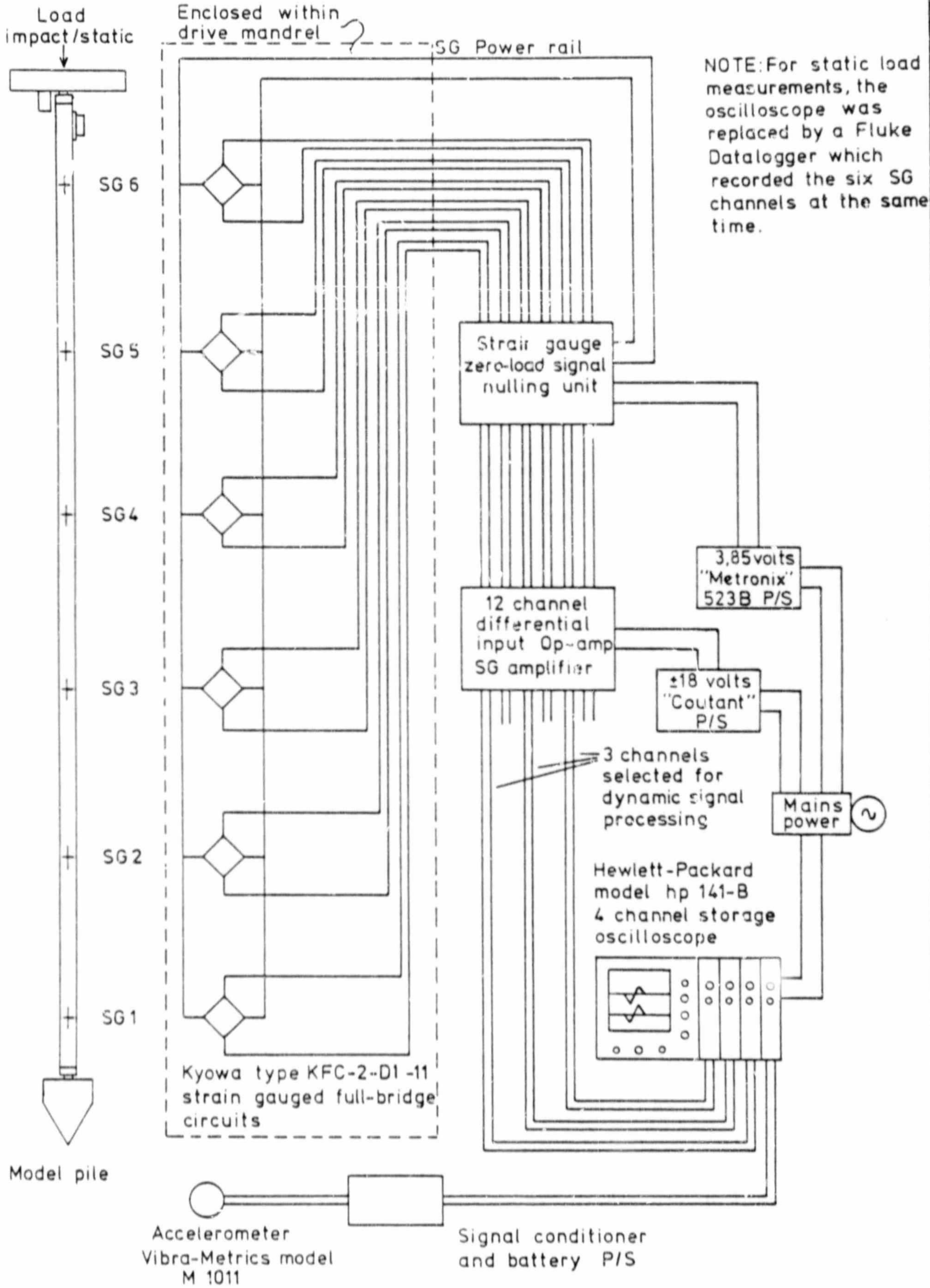

FIGURE 4.8 : Details of the electrical instrumentat
the model pile

complete strain measuring system was checked for stability and frequency/amplitude response in the range 0 - 10kHz and found to be satisfactory for the purposes of the model pile experiment.

A storage oscilloscope, set for a single sweep triggered on receipt of a signal from the accelerometer, was used to record the impact data. Photographs were taken of the signal traces on the oscilloscope screen for later manipulation. During static loading of the piles, the strain gauge signals were recorded on a multichannel datalogger and pile head displacements measured with dial gauges.

Due to a variety of reasons (see for example Sheingold [1980], Vaughan [1975], Dally and Riley [1965], Peekel [1971]), the output signals from strain gauges may drift with time and be subject to interference noise. Where the noise and/or drift was found to be unacceptably high, corrections were applied to the basic strain gauge data to compensate for error induced from these sources.

One of the major developments in experimental soil mechanics of the last three decades has been the emergence of techniques for the visualisation of displacement fields in soil specimens undergoing deformation. The earliest of these methods to have met with success was an X-ray technique, refined by Roscoe et al (1963 a and b), but used previously by Gerber (1929) and Davis and Woodward (1949). Butterfield et al (1970) subsequently proposed a stereo photogrammetric method "... which is suitable for measuring planar displacements of any textured surface." (Butterfield et al, [1972, p. 308]). The method is discussed by Luker (1984), Maddocks (1978) and in some detail by Andrawes (1976).

Soil displacements around the model pile were determined using a version of the stereo photogrammetric technique which corresponds closely to the use of a "stecometer" described by Maddocks (1978). The method is also similar to the use of "the orthogonal displacement meter" described by Roscoe et al (1963a).

As with the stereo photogrammetric technique, the soil pattern around the model pile was recorded on a sequence of photographs. These comprised plate film exposures taken at discrete incremental displacements of the pile using a stationary camera viewing the soil through the glass panel of the sand box. Normally, pairs of photographs are optically superposed in a stereoplotter, and the soil displacements measured by determining the "height" of the resulting stereo-image. The procedure applied here, however, was to measure the co-ordinates of individual sand grains in each photograph. Use of this procedure eliminates the parallax problems which arise in superposition of photo-pairs when significant soil movements occur in two perpendicular directions (refer Luker [1984]). Stationary control points, to which the grain co-ordinates were referred, were provided by a reference grid drawn on the external face of the glass panel. All sand grain displacement diagrams and associated strain diagrams plotted from this data, are located in the rear pocket of this volume.

A Wild A7 Autograph was used to measure the grain co-ordinates (see plate 4.3). Figures 4.9 and 4.10 show the principles of the method which is discussed in detail in Appendix A.

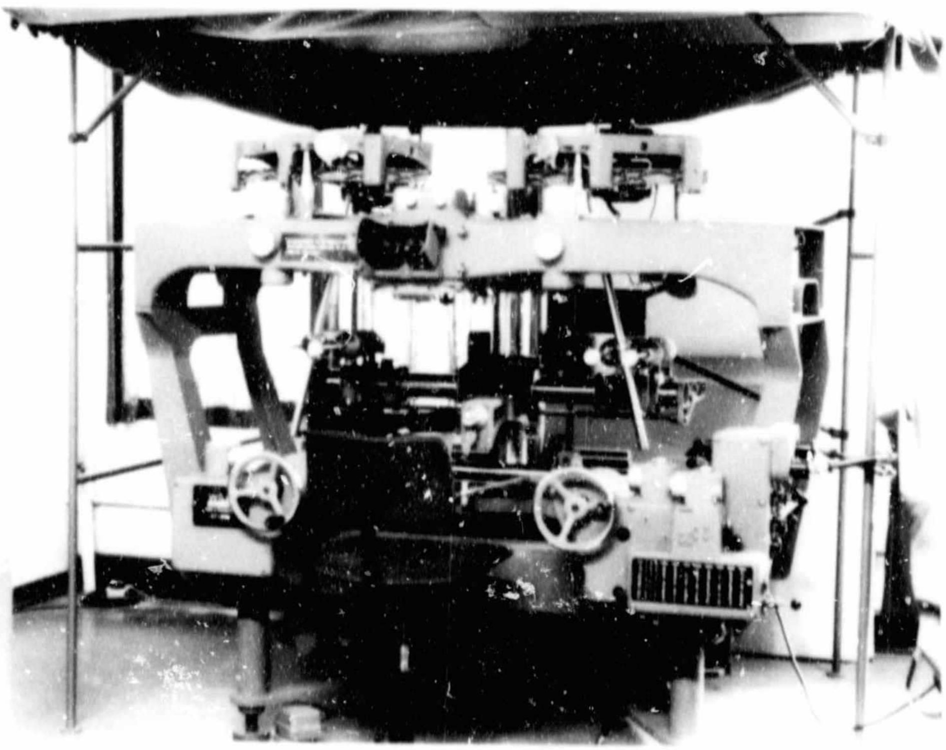

PLATE 4.3 : Wild A7 Autograph

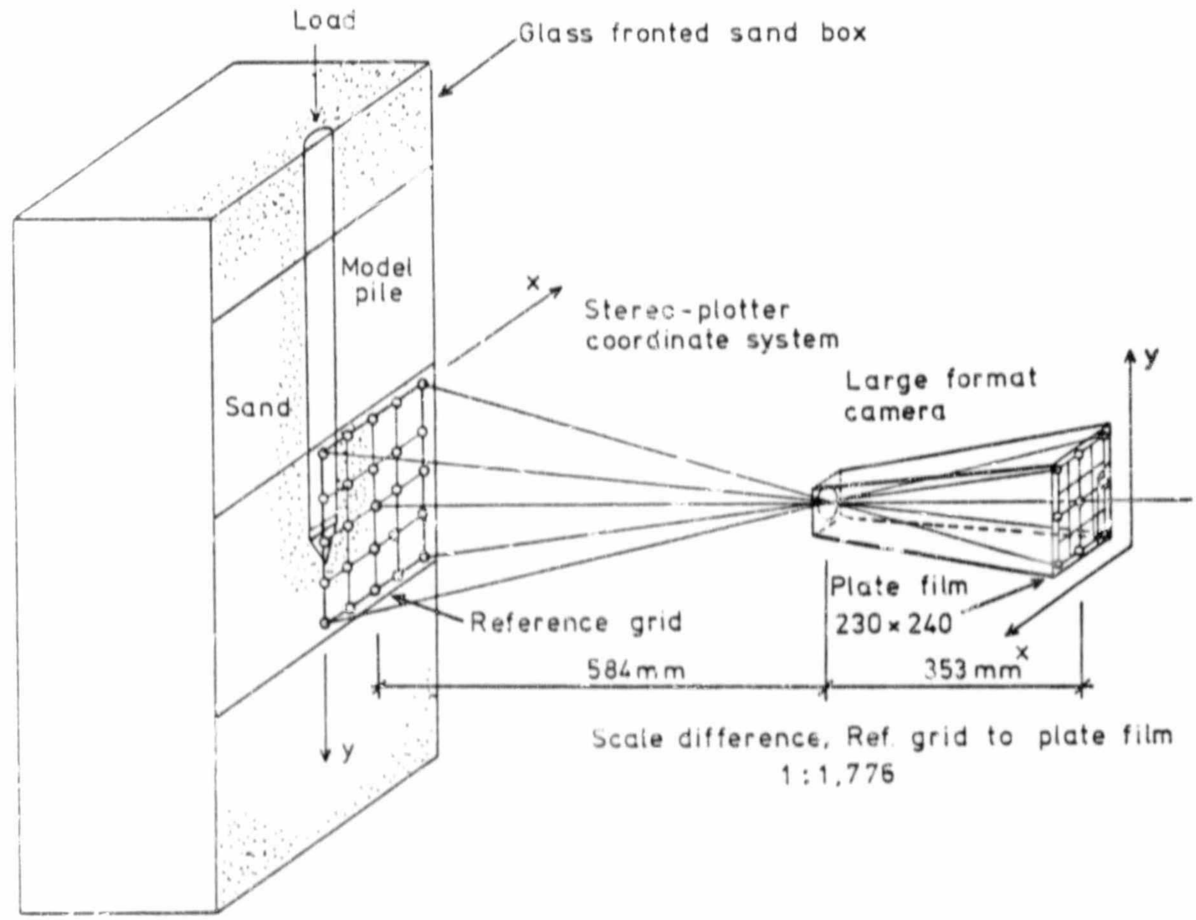

FIGURE 4.9 : Sketch diagram showing the camera, pile soil and reference grid arrangements

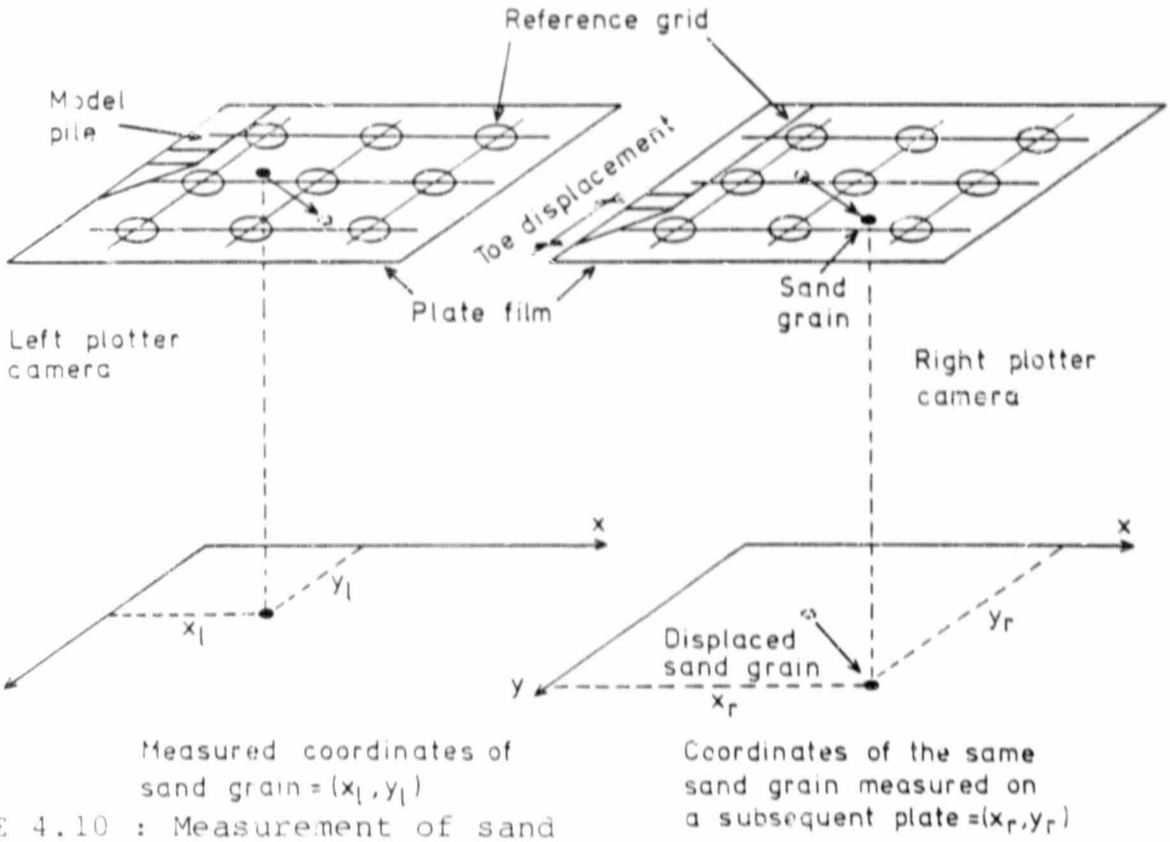

FIGURE 4.10 : Measurement of sand grain displacements in the Wild A7 Autograph

5. EXPERIMENTAL RESULTS

The installation of a model MV pile in the laboratory using the methods and techniques described in Chapter 4 was achieved with sporadic success. The major causes of installation failures included blockage of sand rainer perforations leading to uneven sand placement, blockages in the grout circuit, the pile shoe moving away from the glass panel and the pile shaft bonding onto the glass panel. Of the ten pile installation experiments carried out in the laboratory, two were successful and one of these, the ninth experiment, has been analysed in detail. Most of the test results recorded in this chapter were obtained from the ninth experiment, but data from other tests is referred to as necessary.

During the ninth experiment, the model pile was driven to a depth of about 760mm in a sand with an average dry density of $1673 kg/m^3$. Following impact installation, the pile was pushed a further 32mm into the soil to determine the load developed on the pile shoe. After allowing the grout to cure, the pile was load tested to failure in both submerged sand and subsequently in drained sand. Table 5.1 presents a summary of some of the information gathered during the installation and load testing of the model pile during this experiment.

TABLE 5.1 : Summary of information gathered during installation and load testing of the model pile

Depth of Point of Pile Shoe	Depth Increment	Record Obtained	Type of Event
750,00mm		Plate 1 Dynamic. Penultimate impact record. (see Fig.5.1)	
	5,62mm		Impact installation of pile into submerged sand. Final two impacts.
755,62mm		Plate 2 Dynamic. Final impact.	
	4,29 mm		
759,91 mm		Plate 3 Dynamic.	
	32,00 mm	Toe resistance of pile.	Immediate post-installation static load test.
791,91 mm	0,23mm		Curing of grout.
792,14 mm		Plate 1 Static.	
	0,83mm		
792,97mm		Plate 2 Static.	Static load test on pile in submerged sand.
	1,17mm		
794,14 mm		Plate 3 Static. Load distribution in pile shaft and load/settlement	
	2,85mm		
796,99mm		Plate 4 Static. behaviour.	Water drained off.
	1,48mm		
798,47mm		Plate 5 Static	Static load test on pile in drained sand.
	1,68mm		
800,15 mm		Unload / Rebound	END TEST
			Pile shaft, load-calibrated

Although the strain gauged load measuring system was checked for stability prior to pile installation, both signal noise and drift were detected during the test programme. The major source of signal noise, which affected all the strain gauges equally, was due to the 230V, 50Hz mains power supply. The amplitude of the mains noise remained approximately constant throughout the tests at an equivalent load error of $\pm 9N$ in the drive mandrel, while over the portion of the drive mandrel stiffened by grout, the equivalent load error was $\pm 12N$. Apart from the application of normal screening procedures, no specific attempts were made to filter this noise, and the precision of all static load test data should be interpreted accordingly. Corrections for 50Hz signal noise in the impact loading data given in Figure 5.1 was, however, made by applying graphical adjustments to the oscilloscope trace.

Signal drift was found to be significant in strain gauge groups SG2, SG4 and SG6 during the static load tests. The drift may have developed as a result of damage to the strain gauges during impact installation of the model pile. The drift behaviour of the strain gauge groups was determined by monitoring their output under no load conditions over a 4 hour period on completion of the loading programme. In general, the drift was found to follow an essentially linear trend with time, but to fluctuate within limits. This non-linear component of the drift is given in Tables 5.2 and 5.3 as the accumulated drift error at the end of the respective static load tests.

All the loads given in the following discussion refer to loads determined from the strain gauge data after the application of the corrections for drift and noise as described.

Because both the pile shoe and the plastic grout-to-glass separator strip lay in contact with the glass front panel of the sand box, a portion of the measured loads was due to friction forces developed on this interface. It was therefore not possible with the equipment used to determine directly the load on the pile due to soil resistance alone. An estimate of the possible magnitude of the glass friction load under various conditions are given in Appendix E. Load data given in the following, however, refer to uncorrected loads, as measured, unless indicated otherwise.

5.1 Impact Installation

The oscilloscope traces of the pile head acceleration and mandrel load near the pile toe (at SG 1, see Figure 4.3) recorded as amplitude versus time during the final three hammer blows at the end of the pile installation (ie immediately preceding Plates 1, 2 and 3 Dynamic) are shown in Plates 5.1a to 5.1c. The data of Plate 5.1b, the penultimate hammer blow, has been plotted in Figure 5.1. Also shown in Figure 5.1 are the pile head velocity and displacement which were obtained by integration of the recorded acceleration. Except for differences in amplitude and slope, the osciloscope